Annals of Nuclear Energy 226 (2026) 111890

Contents lists available at ScienceDirect

Annals of Nuclear Energy

journal homepage: www.elsevier.com/locate/anucene

The scaling of turbulent flame acceleration and detonation transition for hydrogen–air mixtures in the RUT facility☆

M. Kuznetsov [a],*, A. Kotchourko [a], K. Ren [a], W. Breitung [b], A.K. Hayashi [c]

[a] Karlsruhe Institute of Technology, Hermann-von-Helmholtz-Platz 1, 76344 Eggenstein-Leopoldshafen, Germany
[b] Pro-Science GmbH, Parkstraße 9, 76275 Ettlingen, Germany
[c] Aoyama Gakuin University, 4-4-25 Shibuya, Shibuya, Tokyo 150-8366, Japan

ARTICLE INFO

Keywords:
Hydrogen
Combustion
Severe accident
Flame acceleration
Detonation transition
Modeling

ABSTRACT

To model the combustion stage of Loss of Coolant Accident (LOCA) in the containment of a nuclear power plant (NPP), a series of large-scale benchmark experiments have been conducted in the RUT facility. Flame propagation regimes for very lean hydrogen–air mixtures from 10 to 14 vol.% H_2 have been investigated in the RUT set-up. The facility consists of three parts: 34-m channel, 10.5-m canyon, 20-m second channel. The total volume of the mixture was about 480 m^3. 30 and 60% of the channel cross-section was blocked by concrete blocks. Slow and sonic deflagrations in the channel have been established for hydrogen concentrations up to 12.5 vol.% H_2, as a detonation transition at 14 vol.% of hydrogen was registered. In a canyon of a bigger dimension, the detonation was observed even at 12.5 vol.% H_2 due to shock reflection at the far corner of the canyon. Such detonable concentrations for channel and canyon geometries confirm the validity of the 7λ criterion for detonation onset, recommended in the NEA SOAR report and significantly extend the conventional concentration detonability limits of 18–59 vol.% H_2 (NASA STD 8719.16 — Safety Standards) commonly used in non-nuclear safety guidelines. Current experimental and numerical data demonstrate a very high risk of detonation even for very lean hydrogen–air mixtures. The scaling down of flame acceleration and detonation transition was investigated for the same geometry in a MINIRUT facility of 50 times smaller size than the original RUT facility confirms the validity of the 7λ criterion in two orders of magnitude smaller scale. The detonation in the channel and in the canyon of a 50 times smaller scale has occurred for hydrogen–air mixtures with a detonation cell size of 50–57 times smaller than for a real-scale RUT facility. The video monitoring confirmed the shock reflection and shock-flame interaction mechanisms for deflagration to detonation transition (DDT). Beyond the detonation cases for leaner hydrogen–air mixtures, the flame can propagate as subsonic or sonic deflagration. The criterion for sonic deflagration will be the critical expansion ratio σ = 3.75, which corresponds to 10.5–11 vol.% H_2. The experiments also confirmed that the flame dynamics for the deflagration mode do not scale down as the DDT process. Only CFD modeling can predict the turbulent flame propagation at different scales.

1. Introduction

Hydrogen release through a leak due to the Loss of Coolant Accident (LOCA) or Molten Corium–Concrete Interaction (MCCI) accident results in the formation of a hydrogen–air cloud inside the reactor building. Delayed ignition of such a cloud, due to the operation of ignitors, catalytic recombiners, or other causes, may lead to hydrogen combustion in different regimes depending on the initial pressure and temperature, hydrogen concentration, geometry, and scale. Under certain initial and boundary conditions, accelerated flames, fast turbulent deflagrations, and transition to detonation may occur. The DDT event and detonation processes are able to produce the most severe damage to the confining structures, similar to the Fukushima-Daiichi accident in Unit 1 and Unit 3 (Yanez et al., 2015; Kuznetsov et al., 2015; Xiao et al., 2017).

Critical conditions for flame acceleration to the speed of sound and then to detonation onset in confined geometry have been experimentally defined and normalized to the scale as "σ" and "7λ" criteria (Dorofeev et al., 2001, 2000; Kuznetsov et al., 2005). These data have been included to NEA reports and recommended for the nuclear society as the common flame acceleration "σ" and detonation

☆ This article is part of a Special issue entitled: 'ERMSAR 2024' published in Annals of Nuclear Energy.

* Corresponding author.
E-mail address: kuznetsov@kit.edu (M. Kuznetsov).

https://doi.org/10.1016/j.anucene.2025.111890
Received 13 April 2025; Received in revised form 4 September 2025; Accepted 12 September 2025
Available online 6 October 2025
0306-4549/© 2025 The Authors. Published by Elsevier Ltd. This is an open access article under the CC BY license (http://creativecommons.org/licenses/by/4.0/).

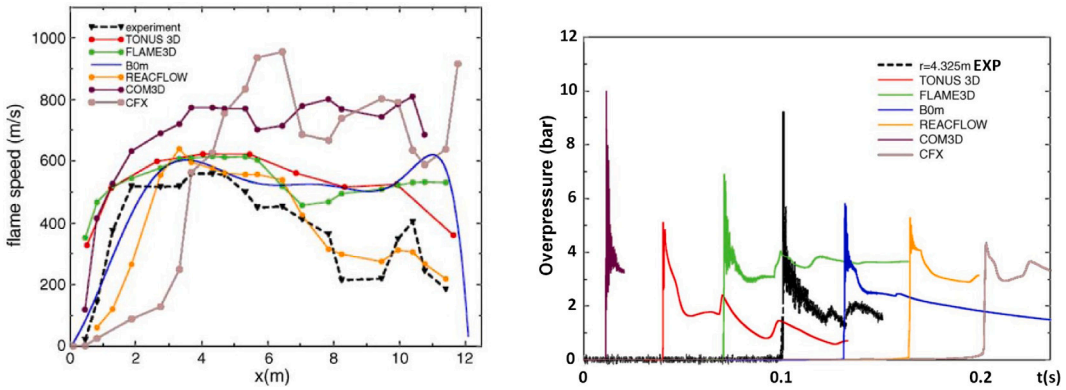

Fig. 1. Comparison of different CFD-code simulations for mc043 experiment with non-uniform mixture (13%H_2 $\Longrightarrow$ 10%H_2): left — flame propagation velocity; right — pressure records at a distance $x = 4.3$ m.

onset "7λ" criteria. Different pressure loads can be expected depending on the flame propagation regime and the strength of the hydrogen explosion. Global pressure loads affect the containment building. The local pressure loads are more sensitive to details of the hydrogen distribution inside the containment, its geometry, venting areas and areas of connecting openings between sub-compartments. It is possible that the global pressure rise remains below a certain safety level limit for containment, but local loads could seriously damage principal containment components, internal walls and/or safety equipment.

The geometrical scale is one of the most important factors that affect the processes of turbulent flame propagation and DDT. Due to this reason, it is always important to have experimental data that explicitly shows the effect of scale and can be used to verify corresponding models of these processes. For example, a large-scale methane explosion in obstructed channels of a coal mine was successfully numerically simulated on two scales using Direct Numerical Simulations (DNS) (Gamezo et al., 2021; Kessler et al., 2010).

The detonability limits for hydrogen–air mixtures from 18% to 59% (vol.) have been declared in the NASA standards (NASA, 1997) independent of the scale of the system. Using large-scale experiments up to a 2.5 m cross-section the detonability limits were extended from 12.5% to 62% hydrogen (Dorofeev et al., 2001, 2000; Kuznetsov et al., 2005).

A substantial database relevant to the hydrogen safety of nuclear power plants (NPP) has been accumulated on the behavior of turbulent flames and DDT conditions in the RUT facility (Moscow region, Russia) at a large scale. These data include a description of the propagation of turbulent flames in the obstructed channel (2.5 × 2.3 × 34 m) with different obstacle configurations, experimental data on the evolution of turbulent flames propagating from the channel to the larger compartment (2.5 × 6 × 10.5 m) and data on the limiting conditions for DDT in these compartments (Dorofeev et al., 1996a,b, 1997). Data have been simulated with different CFD codes only for the deflagrative combustion mode, including turbulent flame acceleration until sonic deflagration (Breitung et al., 2005). The criteria for better agreement between numerical simulations and experimental data were the local flame velocity at different distances (Fig. 1, left) and the arrival time of the strong shock wave to the pressure sensor at a certain position (Fig. 1, right). Since the flame velocity is very sensitive to the turbulence, the overestimated turbulence leads to a faster flame acceleration and to a shorter flame arrival time from the ignition point to the control pressure sensor. Only a few numerical codes REACFLOW, TONUS 3D, and FLAME 3D demonstrated quite good agreement with the experimental data (Fig. 1).

The same RUT geometry was used to simulate the slow and fast deflagration using the EUROPLEXUS code (Velikorodny et al., 2013, 2015). The code is more flexible with respect to the time and scale. The authors tuned the results of the simulations using two turbulence

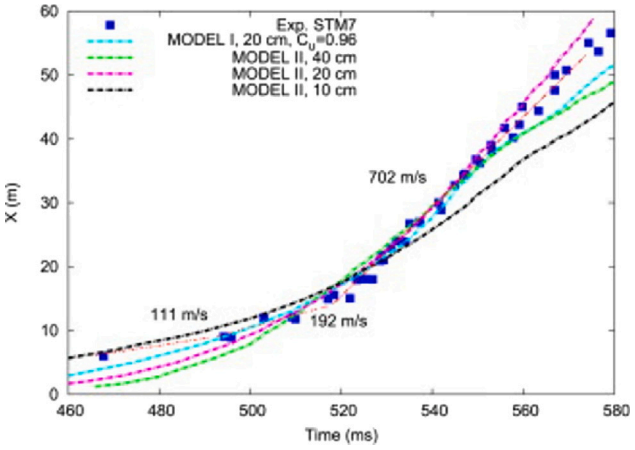

Fig. 2. Comparison of EUROPLEXUS calculation vs. RUT STM7 experiment (17.5%H_2, 25.7%H_2O, T = 362K). Time of arrival — distance (X) diagram depending on turbulence model and mesh size (Velikorodny et al., 2015).

models. In Model I, the turbulent velocity is expressed as a product of several factors. In addition to the turbulence factor defined by Bradley et al. (1992), the model includes the flame wrinkling factor governed by hydrodynamic flame instability (Darrieus–Landau, Rayleigh–Taylor, Kelvin–Helmholtz), leading to an increase in flame surface. It can sufficiently increase the flame rate provided by the pure turbulence. The second model (Model II), which is variable in space and time, was based on the gas velocity field and its gradients. The integral length scale L is dynamically updated in the regions of the elevated vorticity/shear using a local value of the thickness of the vorticity. The time scales in the computation have been adjusted against experiments in order to correct for the initial flame development phase, i.e., the transition from laminar to turbulent flame. Compared to other codes (REACFLOW, TONUS 3D, and FLAME 3D) with very stiff turbulence models insensitive to the scale and time, the EUROPLUXUS code demonstrates much better agreement with experimental data (Fig. 2).

The most challenging problem is numerically simulating the deflagration to detonation transition (DDT). As the simplest case, the direct initiation of detonation experiments in a bent channel connected to the canyon of the RUT facility was successfully simulated in Yáñez et al. (2011), Heidari et al. (2011), Kim and Kim (2019) and Zhang et al. (2019). Compared to the direct initiation of the detonation, the process of DDT is influenced by many physical factors. Among the most important ones is the effect of the scale and geometry. The difficulty in large-scale numerical simulations is that the typical geometrical size of a compartment can be ten orders of magnitude larger than the chemical

Table 1
Initial conditions for RUT facility and main experimental results.

Test #	vol.%H_2	BR %	$S1$ m^2	D_{CJ} m/s	D_{exp} m/s	P_{CJ} bar	P_{exp} bar	Regime
11	12.5	30	2	1405	830	9.1	9.6	D
13	11	30	2	1334	200–500	8.25	5.7	F
15	12.5	30	2	1405	1240–1690	9.1	12.6	D
16	12.5	30	5.6	1405	1360–1650	9.1	14.2	D
17	11	30	5.6	1334	250	8.25	3.5	S
18	9.8	0	1.4	1273	–	7.53	0.9	S
19	12.5	0	5.6	1405	30–40	9.1	1.06	S
20	14	0	5.6	1472	75–80	9.9	2.03	S
21	12.5	60	5.6	1405	350–600	9.1	8.4	F
22	14	60	5.6	1472	1000–1480	9.9	19.1	D
23	12.5	60	5.6	1405	560–620	9.1	3.8	F

Note: D — detonation; F — sonic deflagration (fast); S — sub-sonic deflagration (slow). All combustion properties are calculated using thermodynamic STANJAN code (Reynolds, 1980).

scale that will be used to resolve the DDT process numerically. To do this, mesh refinement should be used, or large-scale experiments must be supplemented by small-scale laboratory studies on turbulent flame propagation and DDT. For numerical code validation, the corresponding numerical and analytical models for flame acceleration, turbulent deflagration, and DDT should describe the effects of scale and should be validated against the large-scale experimental data. For the first time, a 3D CFD code FOCUS-I with Adaptive Mesh Refinement (AMR) and detailed chemistry was successfully applied for numerical simulation of flame acceleration and DDT process in a large-scale RUT facility (Nakamori et al., 2023).

The main goal of this work is an experimental study and numerical simulations on the behavior of turbulent flames and DDT phenomena in two 50 times different scales for the RUT geometry. The small-scale study using the MINIRUT apparatus gives an advantage in resolving the details of detonation onset using high-speed shadow photography, which was not possible to use in the original scale experiments. Then, the results of large- and small-scale experiments can be used more effectively for numerical simulations of flame acceleration and DDT processes.

2. Experimental details

2.1. Large scale experiments

The scheme of the RUT facility is presented in Fig. 3. According to Dorofeev et al. (1996a,b, 1997), the facility consists of three parts. The first part is a long channel of 2.5 × 2.3 m cross-section and 34.6 m length. The second part is a large cavity called a 'canyon' with a cross-section of 6 × 2.5 m and a length of 10.5 m. The third part is a channel of 2.5 × 2.3 m cross-section and 20 m length. The entrance of the facility, at the left end of the first channel, was closed by steel plates of 70–90 tons total mass. Twelve concrete obstacles were placed inside the facility along the first channel spaced by a 2.5 m distance. The blockage ratio was 0%, 30% and 60%. Seven fans were installed inside the facility to mix the gas during the preparation of the mixture.

A series of tests with lean hydrogen–air mixtures has been performed under normal initial temperature and pressure (T = 293K and P = 1bar). The hydrogen concentration varied from 10 to 14 vol.% H_2. Hydrogen concentration and mixture uniformity were measured using 7 acoustic gauges. The mixture was ignited by an electric spark igniter placed at the beginning of the first channel (left end in Fig. 3). The dynamics of flame front and shock wave propagation were monitored using ion probes, pressure transducers, and photodiodes. A list of experiments with initial conditions and main experimental results is shown in Table 1, where the blockage ratio $BR = A_b/A$ is the ratio of blocked area A_b to total cross-section A; $S1$ is the area of the end plate 5 (see Fig. 3); D_{exp} and D_{CJ}, P_{exp} and P_{CJ} are the experimental and theoretical Chapman–Jouguet detonation velocity and pressure. Depending on mixture reactivity and blockage ratio, a slow (S) subsonic deflagration, fast (F) sonic deflagration, and detonations (D) with different combustion velocity and pressure may occur.

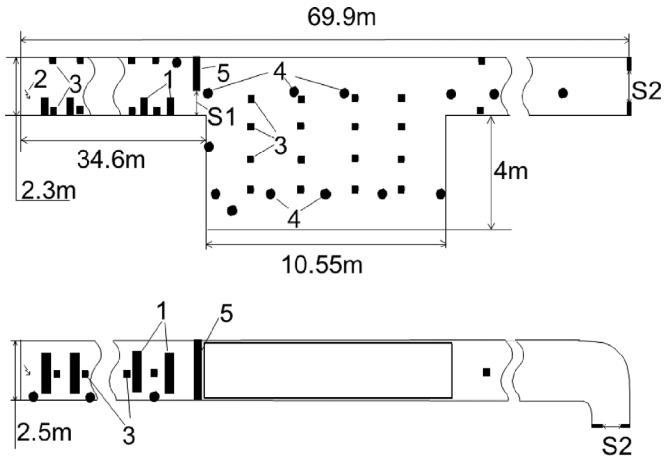

Fig. 3. Scheme of the RUT facility: 1 — obstacles; 2 — ignition position; 3 — light (flame) sensors; 4 — pressure transducers; 5 — steel plate.

2.2. Small scale experiments

Small-scale experiments have been carried out in the MINIRUT experimental apparatus (Kurchatov Institute, Moscow, Russia). Its main dimensions are less than the RUT facility by a factor of 50. The apparatus consists of four sections (see Fig. 4 Matsukov et al., 1999). Sections #2 and #4 correspond to channels of the RUT facility. Sections #2 and #3 are filled with obstacles (blockage ratio BR = 30%) spaced by the size of the channel 2.5 m. The length of each section (about 250 mm) was controlled by the light beam diameter of the Schlieren system.

Each of the sections was equipped with transparent quartz windows for optical observations. Section #1 with dimensions of 211 × 125 × 50 mm corresponds to the canyon of the RUT facility. MINIRUT channel can be elongated by installing additional sections (0.2, 0.6 and 0.328 m) with or without obstacles.

Photodiodes and piezoelectric pressure transducers have been used to record the dynamics of flame and shock front propagation. Since in small-scale experiments, photodiodes and pressure sensors cannot provide detailed information on flame shape, a Schlieren technique was used to monitor detailed information on the development of turbulent flames and explosion processes. Experiments were conducted using a high-speed drum camera SK-2 with 5000 frames/sec.

In the tests, hydrogen–air mixtures with hydrogen concentrations of 22 to 30% and stoichiometric hydrogen–oxygen mixtures diluted with nitrogen ($2H_2 + O_2 + \beta N_2$) were used (Tables 2 and 3). The mixtures were ignited using a high-voltage spark plug located flush to the front cover of the channel. Detonation cell size λ, evaluated with CELL-H2 code (Gavrikov et al., 2000), will then be used in dimensionless

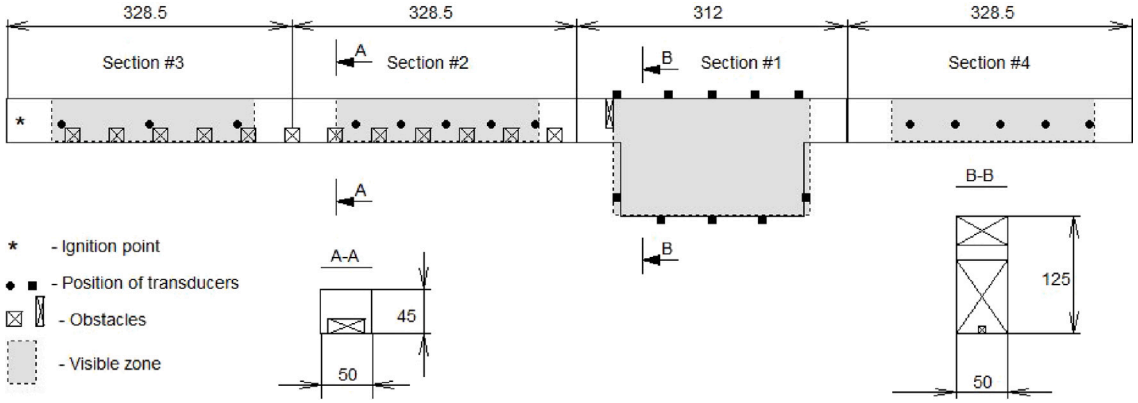

Fig. 4. Schematic of MINIRUT facility: ⋆ — ignition position; ⊠ — obstacles; ■, • — sensors.

Table 2
N2-diluted stoichiometric H2–O2 test mixtures.

Mixture	β	vol. %H_2	vol. %O_2	vol. %N_2	Detonation cell size λ mm
1	3.76	29.6	14.8	55.6	12.0
2	3.6	30.3	15.2	54.6	11.4
3	3.5	30.8	15.4	53.9	11.1
4	3	33.3	16.7	50	9.4
5	2	40	20	40	6.2

Note: $\beta = [N_2]/[O_2]$. Detonation cell size λ is calculated using CELL-H2 code (Gavrikov et al., 2000).

Table 3
H2–air test mixtures.

Mixture	β	vol. %H_2	vol. %O_2	vol. %N_2	Detonation cell size λ mm
1	3.76	29.6	14.8	55.6	12.0
6	3.76	28	15.1	56.9	14.1
7	3.76	27	15.3	57.7	15.1
8	3.76	26	15.6	58.5	16.5
9	3.76	25	15.8	59.2	18.3
10	3.76	24	16.0	60.0	20.8
11	3.76	23	16.2	60.8	24.7
12	3.76	22	16.4	61.6	30.9

Note: $\beta = [N_2]/[O_2]$. Detonation cell size λ is calculated using CELL-H2 code (Gavrikov et al., 2000).

analysis of L/λ ratio to avoid the discrepancy of experimental cell size definition.

3. Experimental results

3.1. Large scale experiments

From the observed experimental results, four typical regimes can be distinguished. Slow subsonic turbulent deflagration was observed in tests 18–20 without obstacles (Table 1). Fast (sonic) deflagration was observed in tests 12,13,17,21,23. DDT in the first channel and further stable detonation propagation was observed in test 22. A regime with detonation onset due to shock wave reflection was observed in tests 14–16. To plot flame front surfaces in a canyon with a constant time step, a third-degree polynomial interpolation was applied for flame arrival times at a certain position of each photodiode. Two-dimensional projections of flame shape, detonation and reflected shock evolution are shown in Figs. 5, 6.

An example of a $X - t$ (distance–time) diagram of the explosion regime with DDT in a channel and detonation onset due to shock reflection in a canyon is shown in Figs. 7 and 8. This diagram shows

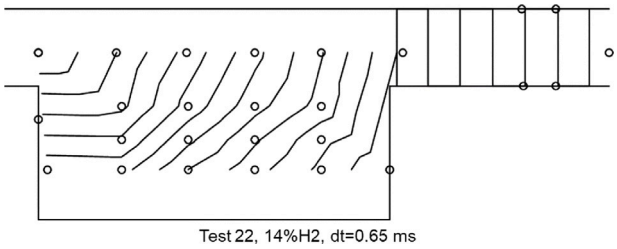

Fig. 5. Detonation front propagation (solid lines) from first channel to the canyon and the second channel. (o) — positions of transducers, time step between iso-lines Δt = 0.65 ms.

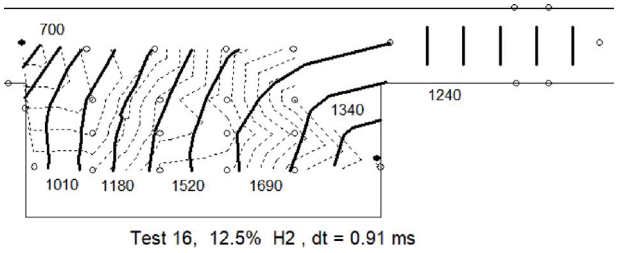

Fig. 6. Flame shapes (dotted lines) and secondary explosion waves (solid lines) for DDT process in the canyon (Test 16, 12.5%H_2). Local velocities of explosion waves in m/s. (o) — locations of transducers, time step between iso-lines Δt = 0.91 ms.

records of pressure–time or simply arrival-time records for sensors at certain distances positioned along the facility. The slope of the line between two sensors corresponds to the characteristic (local) velocity of flame or shock wave propagation ($v = \Delta X/\Delta t$).

Results obtained in a series of large-scale experiments have indicated that flame propagation, pressure build-up and transition to detonation depend on mixture composition, turbulence generation and geometrical scale. The existence of sub-sonic and sonic deflagration within a narrow range of hydrogen concentrations 10%–11% (see Table 1) confirms the critical expansion ratio σ = 3.75 for fast (sonic) flame propagation according to Dorofeev et al. (2001). The mixtures available to accelerate over the speed of sound can detonate, as in the tests 11, 14–16, 22. A significant peculiarity was found that the compositions of 12.5%–14% H_2 in air correspond to lean mixtures, which are not far from the flammability limit. The strength of the detonation process is demonstrated in Fig. 9 by the removal of the channel end door by the 90-ton concrete and metal plates assembly. The total force of the detonation pressure on the exit wall exceeds 20 MN, equal to the weight of 2000 tons.

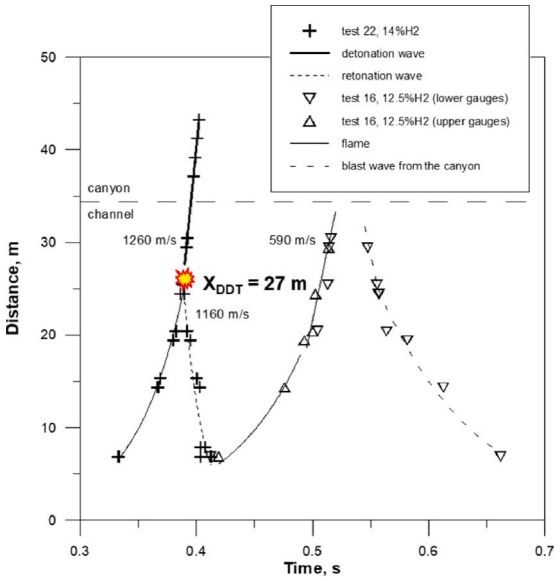

Fig. 7. X–t diagrams of the DDT process in the channel (14%H_2) (left) and canyon (12.5%H_2) (right) based on photodiodes: yellow-red ⋆ — DDT point.

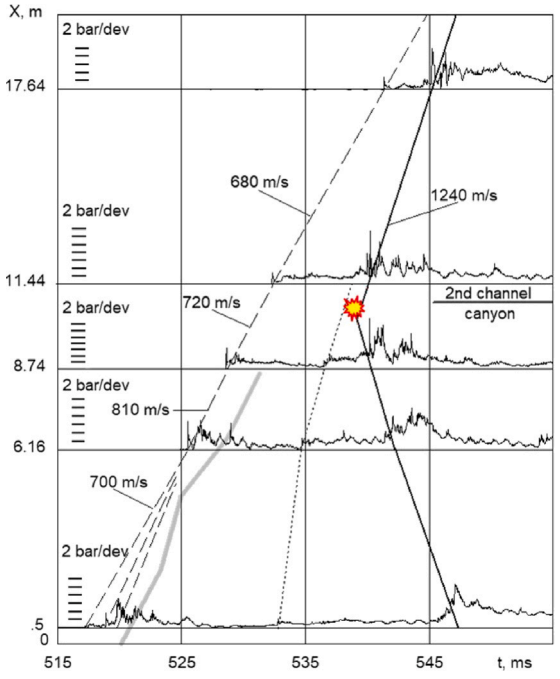

Fig. 8. X–t diagrams of the DDT process in the canyon (12.5 vol.%H_2) based on pressure sensors: yellow-red ⋆ — DDT point. The first channel is not shown.

The transition to detonation was observed at a minimum of 12.5% of hydrogen. Although unstable or deficit-velocity detonations may be expected in such mixtures and geometrical configurations, DDT events were clearly observed and reproduced. It was found that at critical conditions (12.5% H_2) the flame accelerates down the obstructed channel and reaches a quasi-stationary speed of about 600 m/s. This fast deflagration regime is analogous to the choking regime observed in laboratory experiments (Peraldi et al., 1988) when the velocity of the combustion products with respect to the flame was about sonic. Shock and flame interactions with obstacles support this fast mode of combustion. However, they never resulted in the onset of detonation with 12.5% H_2, because the transverse dimensions of the obstructed channel were insufficient. The transition to detonation in the channel was observed at the distance x_D = 27–28 m for a more sensitive mixture with 14% H_2.

3.2. Small scale experiments

Flame accelerations in the channel with obstacles (BR=0.3) were investigated for H_2-air mixtures containing 24–29.6% of H_2 and for H_2-O_2 mixtures containing nitrogen N_2 as diluent with β = 2-3.76. The length of the channel was proportional to RUT's channel in a ratio of 1:50. For hydrogen–air mixtures, the flame speed accelerates to the first obstacle to 25–40 m/s. The ratios of flame speed after the first, third, fifth, and seventh obstacles to the first were equal to 1 : (3–4.5) : (7.5–10) : (15–16). The flame speed achieved the sonic velocity close to the end of the channel at 0.4–0.7 m. The so-called "choking" regimes were established. However, DDT processes were not observed in the channel for hydrogen–air mixtures. Only stoichiometric mixtures cause DDT in the canyon, probably because of shock reflection. To increase the reactivity of the mixture, nitrogen-diluted stoichiometric H_2-O_2 mixtures were tested with β = (2, 3, 3.5, 3.6, 3.76) to reach the onset of detonation. The evolution of the flame velocity for the nitrogen-diluted stoichiometric hydrogen–oxygen mixture is shown in Fig. 8 (left) against a dilution coefficient β. Detonation transitions were observed for mixtures with $\beta \leq 3.5$ in a channel geometry. With mixtures (β = 3.6–3.76), the DDT occurs in the canyon. Experimentally, it appeared that detonations were initiated in the canyon in 75% of the cases for β = 3.6 and in 25% of the cases for β = 3.76. The detonation by shock reflection occurred in the canyon more frequently for these mixtures.

This means that the scaling factor of 1/50 of the RUT scale for flame acceleration to sound speed is not valid for the deflagration mode, and the channel length L = 0.7 m is shorter than the run-up distance, or the reactivity of the mixture is too low for the onset of detonation. To obtain the onset of detonation, the length of the channel was increased by one or more additional sections. To understand the effects of channel length on turbulent flame acceleration, burning velocities were measured for additional sections of different lengths La with or without obstacles. The measurements were made for smooth sections of 0.2 and 0.6 m length and the section of La = 0.328 m with obstacles (BR=0.3). The experimental dependencies of flame velocity versus distance along the channel are presented in Fig. 10 (right). Additional sections allow the flame to accelerate to the higher velocity at which DDT conditions in channel geometry are achieved. The effect of obstacles on flame acceleration in the additional section is very crucial. A series of experiments with additional sections of 0.2, 0.328 (BR = 0.3), and 0.6 m length was conducted to determine the critical conditions for DDT in the channel and canyon space. The mixtures considered in these experiments contained 22–29.59% H_2 in air. The minimum hydrogen concentration in hydrogen–air mixtures at which DDT can be observed was equal to 27%–28% for smooth additional sections of La = 0.2 m or La = 0.6 m length. At the same time, the lower concentration limit of the DDT process in the channel and in the canyon with a section of 0.328 m long (BR = 0.3) was experimentally defined as 24 and 25% hydrogen in the air, respectively. For the same stoichiometric hydrogen–air mixture, a faster flame acceleration in a shorter smooth channel (La = 0.2 m) compared to a longer smooth channel (La = 0.6 m) was found. A shorter smooth channel with a flange or obstacle at the end may promote a shorter run-up distance due to reflected shock interaction with the flame front, leading to much higher flame propagation velocity. A similar phenomenon was demonstrated in tests with a relatively short unobstructed channel (Kuznetsov et al., 2017). The flame initially accelerates, producing advanced shock waves with Mach number M = 1.2-1.7. If the tube is shorter than the run-up distance, the advanced shock wave reflects from the tube end, returns back and interacts with a flame surface, producing a very wrinkled surface due to Richtmayer–Meshkov instability. After such

Fig. 9. Side view of main RUT entrance blockage before/during/after the test.

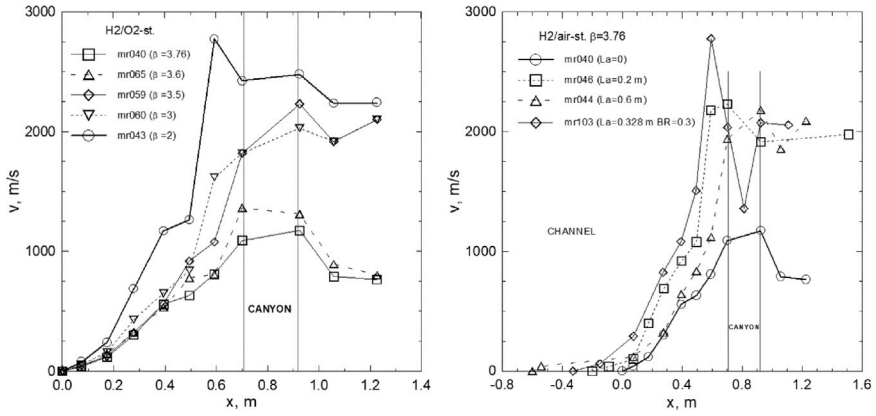

Fig. 10. Evolution of flame speed along the axis: effect of mixture reactivity (left); effect of the channel length due to additional section length *La* (right).

Fig. 11. Schlieren images of flame propagation and DDT process in a channel: left — β = 3.76; right — β = 2.0. The process develops in time from top to bottom, time step $\Delta t \simeq 20$ μs, height of the channel $h = 45$ mm.

interaction, the flame velocity can be ten times higher. It results in a shortening of the run-up distance to DDT several times.

The Schlieren technique with high speed shooting and photodiode measurements was used for a detailed investigation of turbulent flame propagation and interaction with obstacles and following the DDT process. Fig. 11 presents Schlieren photographs of the DDT process in the channel for a stoichiometric mixture with β = 3.76 (left, hydrogen in air) and β = 2 (center, more reactive). It should be noted a particular shape of the flame front for both those mixtures. Two regimes of turbulent flame propagation through obstacles were observed. In the first case (β > 3), the flame preferentially propagates at the top of the channel, avoiding the obstacles (Fig. 11, left). In the second case,

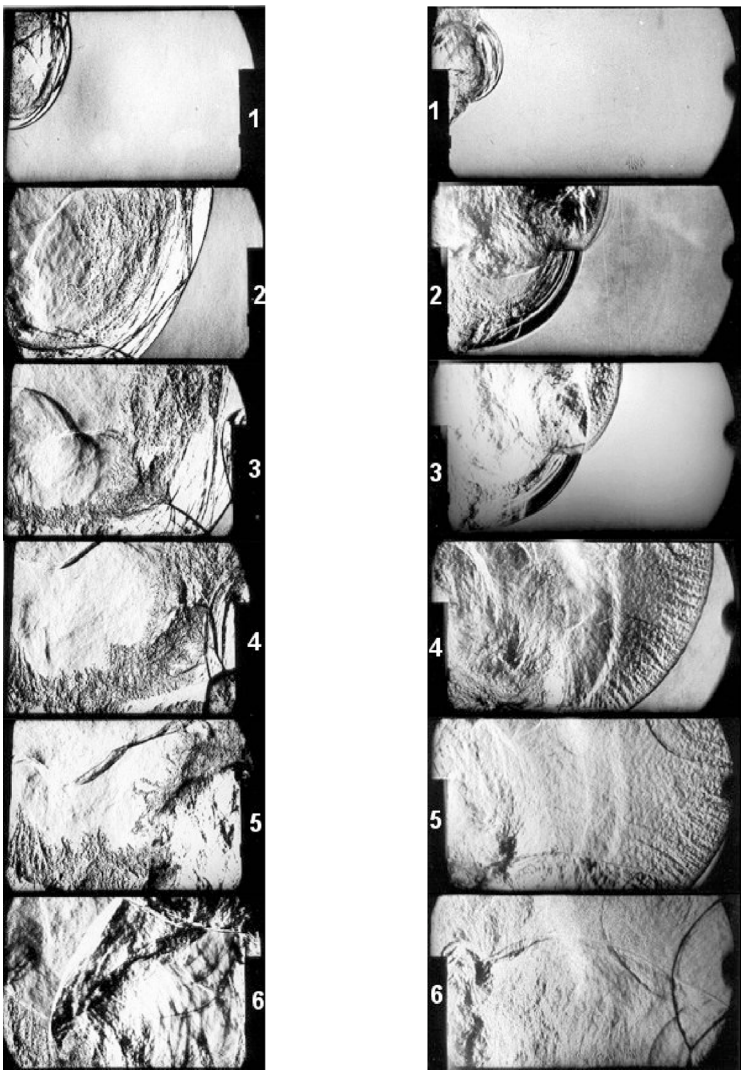

Fig. 12. Schlieren images of the DDT process in a canyon: left, 24%H2–air, DDT at the far end reflection, right, stoichiometric hydrogen–air mixture, DDT due to Mach reflection. The process develops in time from top to bottom, time step $\Delta t \simeq 20$ μs, height of the canyon $h = 125$ mm.

typical of the "fast" mixtures ($\beta \leq 2$), the flame propagates at the bottom through a gap between obstacles and a side wall (Fig. 11, right).

In both cases, an advancing shock wave follows ahead of the flame front at a distance of 15–20 cm. Then, a very intense reflected shock wave is generated by the reflection of the leading shock wave from the obstacle, interacting with the flame and intensifying it due to wrinkling. Then, the complex shock-flame propagates for a long distance with a velocity close to the speed of sound in combustion products (about 1000 m/s). If the length of the channel is sufficient for flame acceleration, detonation can occur in the channel, close to the exit to the canyon, at a distance of about 522 mm from the ignition point. If the length is not enough, the complex shock-flame exits the canyon and then can detonate due to Mach reflection for the 'fast' mixtures or due to the interaction of reflected shock waves at the far corner for hydrogen–air mixtures 24%–26% H_2 (Fig. 12, left).

Another example of DDT in the canyon is shown in Fig. 12 (right). Such a regime occurs for the stoichiometric hydrogen–air mixture. The exit of the first channel was partially blocked at the top part of the channel. The specific shape of the leading shock entering the canyon is shown in the first frame (Fig. 12, right). A Mach reflection of the lead shock from the ceiling results in a strong local explosion and a detonation wave development. The detonation wave propagates without decay through the unburned material. Processes of such type were not observed in the RUT tests, probably because of the difference in the relative sensitivity of the mixtures to the scale.

4. Experimental data analysis and numerical simulations of DDT

4.1. Scaling analysis

The application of experimental results to a wider range of initial conditions and geometrical sizes requires the experimental validation of theoretical models for DDT scaling. Thus, the predictive computer tools describing all combustion regimes, including DDT and detonation propagation, were developed and then validated against experiments to estimate the critical DDT conditions necessary for practical accident analyses. The critical conditions for DDT observed in current tests will be analyzed in terms of the detonation cell size λ as a measure of detonability. The possibility of detonation initiation in a given mixture of cell size λ is limited by a characteristic geometrical size. Experimental data for different fuel–air mixtures show a good agreement with the 7λ — criterion over a wide range of compositions and scales.

The scaling of DDT conditions in the RUT facility to a small-scale experimental apparatus gives an estimate for critical detonable mixture compositions using the 7λ-criterion (Dorofeev et al., 2000, 1996a). For instance, the critical mixture in which DDT occurs in the channel

Table 4
N2-diluted stoichiometric H2–O2 mixtures.

Geometry	Characteristic size L, mm	Critical cell size λ, mm	H_2 concentration (predicted) % H_2 (vol.)
Channel (section #2-#3):			
BR=0.3, spacing 1D	125	~ 18	24% H_2/air
BR=0.6, spacing 2D	75	~ 11	$2H_2+O_2+ \beta N_2$ (β=3.2)
Canyon (section #1)	165	~ 23	22% H_2/air

Note: $\beta = [N_2]/[O_2]$. Detonation cell size λ is calculated using the CELL-H2 code (Gavrikov et al., 2000).

Table 5
Critical cell widths for DDT.

Geometry	RUT	MINIRUT	$\lambda_{RUT}/\lambda_{MINIRUT}$
	λ, mm		
Channel	900	18	50
Canyon	1200	21	57

Note: $\beta = [N_2]/[O_2]$. Detonation cell size λ is calculated using CELL-H2 code (Gavrikov et al., 2000).

of the RUT facility has a detonation cell size of about 1 m. This means that the mixture with λ close to 20 mm is expected to be critical for the MINIRUT facility. Thus, mixtures close to stoichiometric hydrogen–air (β = 3.76) can detonate. Similarly, the critical cell size for the case of DDT in the canyon could also be estimated using a CELL-H2 code (Gavrikov et al., 2000). The compositions of the near-critical mixtures estimated for small-scale experiments in $H_2/O_2/N_2$ mixtures are presented in Table 4. The validity of DDT scaling is also experimentally confirmed by the physical similarity of the DDT process in an obstructed channel (Figs. 5 and 11) and in a canyon geometry (Figs. 6 and 12). This means that the mechanism of detonation onset remains the same, independent of the scale.

A comparison of experimental data on RUT and MINIRUT experiments with respect to the detonation cell size of critical mixtures to be detonated confirms the 7λ criterion very well (Tables 4 and 5). This follows from the exact geometrical scaling and the ratio of detonation cells $\lambda_{RUT}/\lambda_{MINIRUT}$. This is an experimental confirmation of the scale-dependent character of detonability limits, which are in strong contradiction with the well-known detonability limits 18–59%H_2 in air declared in the NASA hydrogen safety guideline (NASA, 1997). Based on our findings, the detonability limits for hydrogen–air mixtures should be extended at least to 12.5%–62% H_2 in air for characteristic size up to 10 m (Dorofeev et al., 2001, 2000; Kuznetsov et al., 2005).

4.2. Run-up distance requirements

To satisfy the DDT scaling down well, it needs to increase the length of the channel in 50% to successfully accelerate the flame to support the onset of detonation (see Fig. 10, right). Keeping the exact geometry scaling factor, without a channel elongation, it should be a more reactive mixture ($2H_2 + O_2$ diluted with N_2, $\beta = 2 - 3.5$) to provide an onset of detonation in a channel (Fig. 10, left). Then, the ratio $\lambda_{RUT}/\lambda_{MINIRUT}$ = 80–90 or L/λ = 10–12.5 (much larger than L/λ = 7). It is caused by different scaling factors of detonation and deflagration processes.

Two major conditions for detonation onset have been formulated in Moen et al. (1980) and Chan (1995): (1) the turbulent flame should accelerate to 500–1000 m/s (or to Mach number M = 1.5) to create the conditions for DDT; (2) the accelerating flame should be able to generate a shock wave with Mach number 2.25 or higher. Such conditions will be sufficient to ignite the mixture in reflections and generate a local explosion leading to detonation (Chan, 1995). To satisfy such conditions, the run-up distance of the accelerating flame must be long enough. The length of this path depends on the level of turbulence produced by the flow ahead of the flame. Higher roughness or congestion of the channel leads to a decreased run-up distance to the detonation onset x_D. In a smooth channel, the run-up distance $x_D = 500\lambda$ (Kuznetsov et al., 2005). The wall roughness and congestion of the channel may significantly reduce the run-up distance to detonation. A very rough estimation according to Kuznetsov et al. (2022) gives the run-up distance $x_D = 200\lambda$ for an obstructed channel with BR = 0.1; $x_D = 160\lambda$ for BR = 0.3; $x_D = 130\lambda$ for BR = 0.6. Such speculations show that the scaling of run-up distance to detonation onset is unpredictable and needs special efforts involving numerical simulations to properly predict the run-up distance.

4.3. Small-scale MINIRUT modeling

The proper numerical simulation of the DDT process requires an experimental database to validate the existing combustion models, taking into account the turbulence and flame instability leading to abrupt flame acceleration and DDT transition. Two small-scale experiments with stoichiometric hydrogen–air mixtures (mr046 and mr044) on detonation onset in the first channel of the MINIRUT setup were simulated with the COM3D CFD code (Kotchourko et al., 2015). Currently, the LMR (local mesh refinement) technique has been implemented in the COM3D code, specifically in the RANS model and Navier–Stokes DNS method, resulting in significantly higher calculation efficiency. However, such a method has some limitations as the requirement for high resolution. The resolution of 0.5 mm was used in the computational domain because both the LES model and Arrhenius method have resolution requirements. For DDT simulation, the hybrid DDT chemical reaction model compares the combustion rate due to the deflagration process ω_{def} with the combustion rate of the detonation ω_{det} for those cases in which the combustible gases have been exposed to detonatibility conditions for a time larger than the corresponding induction time (Gaathaug et al., 2012):

$$\omega = \max(\omega_{det}, \omega_{def}) \tag{1}$$

The reaction rate due to deflagration has been calculated with a modified Gradient mechanism (Lipatnikov and Chomiak, 2002),

$$\omega_{def} = \frac{S_t \rho}{\rho_u} \nabla f \tag{2}$$

where f is the progress variable, and u stands for unburned gas, S_t is the turbulent velocity

$$S_t = S_l + \frac{u'}{\sqrt{1 + \frac{1}{Da^2}}} \tag{3}$$

where S_L is the laminar flame velocity, u' is the velocity of turbulent pulsations, and Da is the Damkoeler number. The progress variable f for deflagration regime is the dimensionless factor, changing from 0 to 1, that characterizes reaction progress until equilibrium is reached or some component is fully depleted. The reaction rate for the detonation has been estimated in Arrhenius form for the cases in which the progress variable c is larger than 1

$$\omega_{det} = \begin{cases} 0 & (c < 1) \\ k \exp(-\frac{E}{RT}) & (c \geq 1) \end{cases} \tag{4}$$

The values chosen for the stoichiometric mixtures were E/R = 8736 K and $k = 1.5 \times 10^7\ s^{-1}$. As shown by the reaction rate of detonation, the switch in reaction rates in DDT simulation depends on

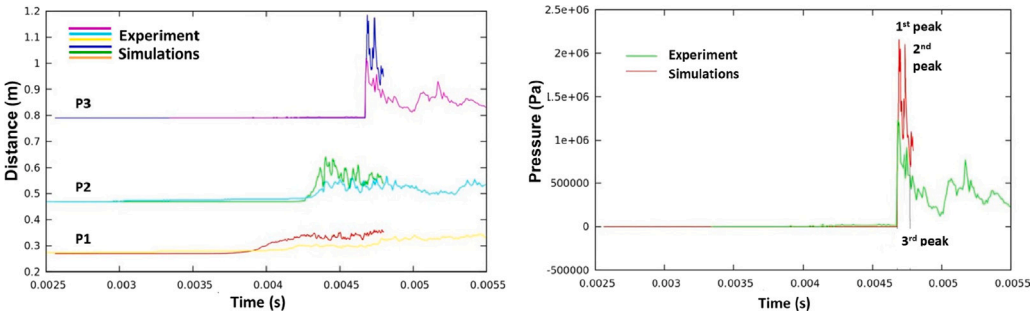

Fig. 13. The $X-t$ diagram of pressure signals (left); comparison of experimental (green) and calculated (red) pressure signals P3 at a distance 0.79 m (right): test mr046 (stoichiometric hydrogen–air, $La = 0.2$m.

the detonation progress variable c, which works as a switch between deflagration and detonation mode and is determined by the induction time as follows:

$$\frac{dc}{dt} = \frac{1}{\tau_{ind}} \tag{5}$$

The methodology requires the knowledge of the induction time in each control volume and time step during the calculation. The induction time has been calculated using the Cantera code (Goodwin, 2009). In the numerical simulation, the deflagration transits to detonation at the last obstacle of the obstructed channel, which is compatible with the results of the MINIRUT experiments (mr046 and mr044). The following part is focused on the comparison of pressure results at three pressure sensors, $X-t$ diagram based on pressure measurements (Fig. 13), and the velocity–distance $v-X$ diagram (Fig. 14) against numerical simulation to validate the CFD code.

Fig. 13 (right) shows the comparison of pressure at the transducer P3 located at 0.79 m, which is near the transition point. According to the experimental results, the combustion mode at P3 is the detonation. Shown in the figure, the numerical simulation reproduces the trend of the pressure curve in MINIRUT experiment mr046 (stoichiometric hydrogen–air mixture), especially in the stages of the second and the third peak. In the comparison of pressure values, numerical results show a large difference vs. the experimental results. The difference in pressure values at P3 is caused by the low spatial resolution of the pressure sensor, rather than the numerical resolution and due to low energy losses in code COM3D. In general, numerical results obtained by COM3D show good agreement with the real experimental results with respect to arrival time.

Fig. 13 (left) shows the so-called $X-t$ diagram of the pressures. Zero line of each pressure record corresponds to their position along the MINIRUT channel. In the figure, a comparison of pressure signals between the numerical simulation and MINIRUT experiment is made in general. From the figure, some details, such as the propagation of pressure waves and the propagation of reflecting waves, are expressed clearly. The figure also demonstrates a very good consistency of calculated and measured pressure signals with respect to the pressure profile and shock wave velocity or arrival time. The detonation onset near sensor P3 happens at the same moment in numerical simulations and experiments. It confirms an adequate model of flame acceleration and the detonation transition of the COM3D code. It even allows for the numerical reproduction of the motion of a real pressure wave.

As shown in Fig. 10, the flame accelerates in an obstructed channel until the speed of sound in combustion products ($v \simeq 1000$ m/s). Then, suddenly, the flame jumps to detonation due to reflected shock-flame interaction (see Fig. 11, left). The strength of the advanced shock wave should be strong enough to initiate the local explosion under reflection from the obstacle, leading to the onset of detonation. Since the strength of the advanced shock wave depends on flame velocity, the level of flame velocity should be of the order of the speed of sound in combustion products to produce a strong enough shock wave of 5–8 bar.

Fig. 14 shows the velocity–distance $v-X$ diagram of the numerical simulations for two experiments, mr046 and mr044 performed in the MINIRUT facility. In the diagram, the horizontal axis is the distance to the ignition point and the vertical axis is the velocity of the flame. The $v-X$ diagram shows the entire flame acceleration process. A comparison between the flame acceleration process of numerical simulation and the flame acceleration process in the experiments shows that the numerical simulation can accurately reproduce the experiments.

Generally speaking, numerical reproductions of the two DDT experiments in the MINIRUT facility are very successful. In the simulation, the numerical reproductions of two DDT experiments under the assistance of the hybrid DDT combustion model look very consistent and reliable with the experiments. The main criteria for the reliability of the numerical simulations were an excellent agreement of arrival time for the flame front and the same run-up distance to the DDT as in the experiments.

4.4. Large-scale RUT modeling

Another example of numerical simulation has been performed for the large-scale RUT facility with a mixture of H2/air using the 3D CFD code FOCUS-I (developed by AdvanceSoft company) (Nakamori et al., 2023; Koike and Matsubara, 2019). For the DDT simulation, the three-dimensional compressible Reynolds-averaged Navier–Stokes equations are solved with 9 species and 21 elementary reactions for the H2–air reaction mechanism. The cell-centered Finite-Volume method is used for discretization. The G-equation is used for the combustion model. The present code takes into account the following processes: mild ignition, laminar flame propagation, wrinkled flame propagation, turbulent flame propagation, DDT, and detonation. Initially, in this 'mild ignition', a laminar flame appears without turbulence. The laminar flame develops, pushing a flow ahead of the flame. Since compressibility exists, compression waves come out from the flame front, and then the Reynolds number grows slightly. Then, the flame front becomes wrinkled, generating many vortices. The Reynolds number becomes larger (up to $Re = 10^5$). In front of the flame, the turbulence becomes stronger, and the flame propagates faster. A time-dependent self-similar law of turbulent combustion (SSLTC) is applied for the turbulent model:

$$SSF = S_{L0} C_g \left(\frac{\rho_u}{\rho_b}\right) \sqrt{\frac{t + t^\star}{\kappa}} \tag{6}$$

where

$$t^\star = \frac{\kappa}{[S_{L0} C_g (\frac{\rho_u}{\rho_b})]^2} \tag{7}$$

where S_{L0} is the laminar flame velocity, κ is the thermodiffusivity, ρ_u and ρ_b are the densities of the unburned and burned material, C_g is the tuning parameter. In addition to SSLTC, Dinkelacker's wrinkling factor for velocity amplification due to an increase in flame surface is

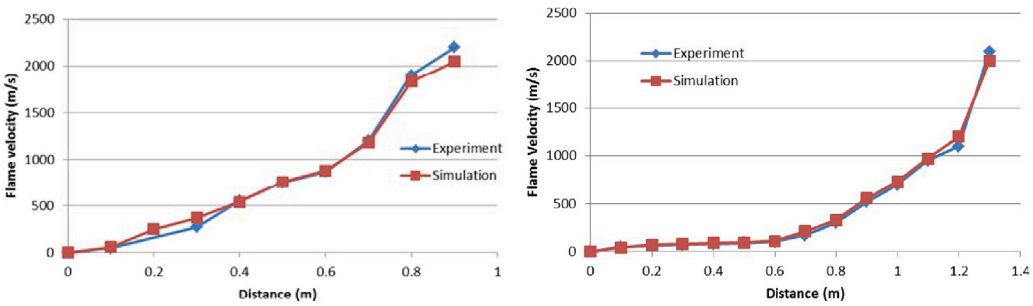

Fig. 14. The $v - X$ diagram of flame propagation velocity in an obstructed channel: left — MINIRUT test mr046 (La = 0.2m); right — MINIRUT test mr044 (La = 0.6m).

developed as a function of the numbers of Lewis (Le) and Reynolds (Re) as follows (Dinkelacker et al., 2011):

$$\Xi = 1 + \frac{0.46}{Le} Re_t^{0.25} \left(\frac{u'}{S_{L0}}\right)^{0.3} \left(\frac{p}{p_0}\right)^{0.2} \tag{8}$$

The Ettner's ignition delay time model (Hasslberger et al., 2015) is used for the detonation transition model. The ignition delay time data table is obtained using the Cantera code (Goodwin, 2009). The time step is about 1 μs, and the grid sizes using the AMR method are between 2.5 cm and 20 cm, depending on the combustion condition, and the total grid number is about 3.76 million.

In the present study, the DDT process in the large real-size combustion tunnel of 34.6 m length and 2.3 × 2.5 m^2 cross-section of RUT22 uses several physical models in order to validate the program for further simulation. Two important points are made clear for the development of the code: the first is that researchers must set a correct configuration of the ignition system and the second is that they must not use the simple initial and boundary conditions but use appropriate physical models based on the DDT physics. It was figured out to set up the program for simulations: (1) The real experimental system has many spaces between obstacles and walls. The authors set up the grid formations based on those fine spacings in the experimental system; (2) The numerical system for DDT has at least six processes. The numerical results we obtained provide a good match with the experimental results.

To visualize the combustion processes in the RUT facility, a small-scale MINIRUT facility in a 1:50 scale was fabricated. Then, the results of 3-D numerical simulations on flame acceleration and DDT in the channel in a real RUT scale (Nakamori et al., 2023) can be compared with small-scale experiments. The comparison demonstrates a very good qualitative agreement with respect to flame shape, shock wave diffraction and reflection, shock-flame interaction and other processes leading to flame acceleration and detonation transition in the channel (Fig. 11). To be consistent on a larger scale, the reactivity of the mixture was established as for a 14% H_2-air mixture. Numerical simulations show that the flame velocity continuously grows to the speed of sound in combustion products v = 500 – 700 m/s, then suddenly the velocity jumps to the detonation with D_{exp} = 1500 m/s. There is some difference between the calculated and experimental detonation velocity D_{exp} = 1260 m/s (see Figs. 7(left) and Table 1. In reality, the detonation velocity deficit may reach 25% of the theoretical value due to energy losses in an obstructed channel with blockage ratio BR = 60% (Dorofeev et al., 2001).

A comparison of real experimental data for RUT and MINIRUT facilities with a rough estimation gives a 50% longer real run-up distance because the detonation cell size is not an appropriate scaling parameter for turbulent flame acceleration. Except for numerical simulation, another scaling parameter should be defined for turbulent flame acceleration and run-up distance to DDT in an obstructed channel geometry. The same problem was encountered during the numerical simulation of the pre-detonation part in the obstructed channel (Nakamori et al., 2023). It was found that the flame acceleration in such a geometry can be divided into two parts: quasi-laminar flame self-acceleration before obstructions due to hydrodynamic flame instability (Darrieus–Landau, Rayleigh–Taylor), leading to flame wrinkling and an increase in the flame surface; and turbulent flame acceleration in the obstructed part. By adjusting the calculated run-up distance with a wrinkling factor, it is brought into alignment with the experimental value of x_D = 27–28 m (Fig. 15). With a very small wrinkling factor, the channel length can even be too short to accelerate the flame to the speed of sound and promote the DDT in a channel (see the red line in Fig. 15 (right)).

Fig. 16 demonstrates an appropriate qualitative consistency of numerical simulations with FOCUS-I for the RUT22 experiment with Schlieren images of flame acceleration in a MINIRUT channel Fig. 11. Since the brightness of Schlieren images is proportional to the density gradient, the higher temperature in Fig. 16(left) somehow corresponds to a brighter region in Fig. 11. Similar to that, since the turbulent flame velocity is proportional to the wrinkling factor, the flow velocity and the strength of the shock wave in Fig. 16(right) are also as strong as the brightness of Schlieren images in Fig. 11. Numerical simulations confirm the preferential flame propagation at the bottom part with a more blocked part of the channel cross-section. Fig. 16(right) shows that as soon as the shock wave is strong enough to ignite the mixture in reflection at the obstacle at a distance of about 27 m, the detonation may occur. The strength of the shock wave depends on turbulent flame velocity, which is proportional to the wrinkling factor (Fig. 16, left).

As one can see, the scaling of the turbulent flame propagation cannot be made with the detonation cell size λ. For a laminar flame (small Reynolds number), other mixture properties, such as laminar burning velocity S_L, expansion ratio σ, etc., should be taken into account (Kuznetsov et al., 1999). If the burning velocity and sound speeds in combustion products c_{sr} and reactants c_{sp} are chosen to give a range of characteristic velocity scales, the corresponding range of the Reynolds number Re may be defined. Variations of these velocity scales for typical fuel–air and fuel–oxygen mixtures cannot compensate for the difference in characteristic length scales (50 times smaller) to provide a similar range of the Reynolds number for turbulent flame propagation. Such an attempt was made using numerical simulations with the FOCUS-I CFD code by a wrinkling factor as a measure of hydrodynamic flame instability. However, a direct comparison of the behavior of turbulent flames in similar geometries and at different scales is important for the verification of turbulent combustion models.

5. Summary and conclusions

The results of an experimental study on flame acceleration and deflagration to detonation transition in RUT geometry of two orders of magnitude difference are presented. The acceleration of flame in a channel with multiple obstacles (BR = 0.3 and BR = 0.6) and the critical conditions for DDT in the channel and canyon geometries have been investigated.

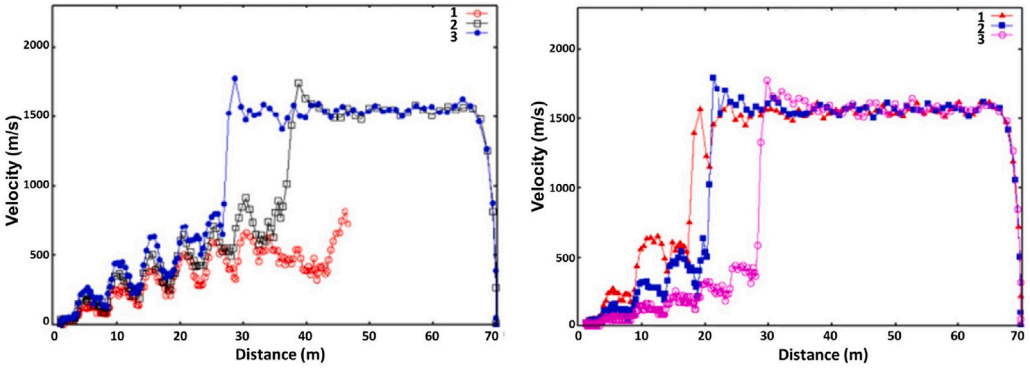

Fig. 15. Numerical simulation of the DDT process in a channel with 14%H2–air: self-similar law of turbulent combustion (SSLTC) model: 1 — $C_g = 0.001$, 2 — $C_g = 0.015$, 3 — $C_g = 0.02$; (left); SSLTC + wrinkling model: 1 — $C_g = 0.02$, 2 — $C_g = 0.009$, 3 — $C_g = 0.002$ (right).

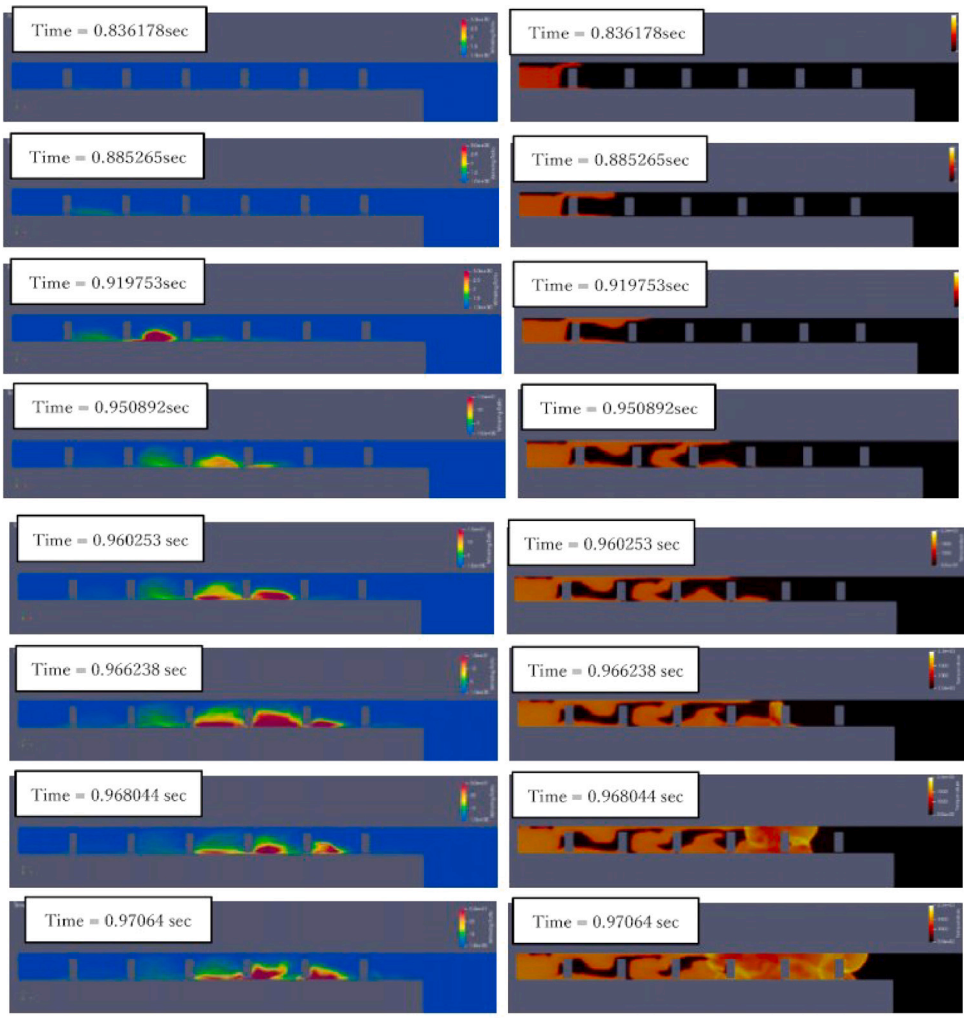

Fig. 16. Simulated wrinkling factor (left) and temperature (right) profiles during DDT process in a channel: 14% H_2-air mixture.

The shadow photographs in the MINIRUT facility permitted us to resolve in some detail the processes of turbulent flame propagation and DDT in a complex RUT geometry. Their comparison with the data from the real RUT tests showed that not only the critical conditions but also the detailed picture of the processes of the onset of detonations are similar if the geometry is scaled with detonation cell size λ. The scaling down in two orders of magnitude compared to the original RUT dimensions confirmed the validity of the 7λ criterion for detonation onset in a channel and multi-room geometry. The cell sizes λ of these critical compositions were found to be exactly 50 times smaller than those for large-scale tests in the RUT facility.

The detonability limits for hydrogen–air mixtures were found to be 14%H2 for the channel and 12.5% H_2 for the canyon geometry. In general, the canyon geometry can be assumed as an elementary cell between two obstacles for an obstructed channel of 6.5 m height blocked in 60%. Then the global detonability limit for hydrogen–air mixtures should be reduced to 12.5% H_2 compared to 18% H_2, according to NASA's hydrogen safety guidelines.

For the first time, two 3D CFD codes, COM3D and FOCUS-I with Adaptive Mesh Refinement (AMR) and detailed chemistry, were successfully applied for numerical simulation of flame acceleration and the DDT process in a channel geometry RUT facility in two very different scales. As shown in numerical simulations, the turbulence plays an important role in flame acceleration to the speed of sound and hydrodynamic flame instability at the initial stage of the combustion process. It needs special efforts to modify the turbulence model to adjust the flame dynamics and run-up distance to experimental values.

A comparison of experimental data on flame acceleration and run-up distance to DDT for RUT and MINIRUT facilities shows that on a smaller scale, it needs 50% longer run-up distance than according to the geometry scale. It means that the detonation cell size is not an appropriate scaling parameter for turbulent flame acceleration. Other scaling parameters should be determined (including Reynolds number) for turbulent flame acceleration and run-up distance to DDT in an obstructed channel geometry.

CRediT authorship contribution statement

M. Kuznetsov: Conceptualization, Formal analysis, Investigation, Writing – original draft, Writing – review & editing, Visualization, Supervision. **A. Kotchourko:** Conceptualization, Investigation, Writing – review & editing. **K. Ren:** Formal analysis, Investigation, Writing – original draft, Visualization. **W. Breitung:** Conceptualization. **A.K. Hayashi:** Conceptualization, Formal analysis, Investigation, Writing – original draft, Visualization, Supervision.

Declaration of competing interest

The authors declare the following financial interests/personal relationships which may be considered as potential competing interests: Mike Kuznetsov reports was provided by Karlsruhe Institute of Technology. If there are other authors, they declare that they have no known competing financial interests or personal relationships that could have appeared to influence the work reported in this paper.

Acknowledgments

The authors are very grateful to our German and Japanese colleagues Dr. Aleksander Lelyakin, Prof. Nobuyuki Tsuboi for their significant contribution and very useful advices. All authors have read and agreed to the published version of the manuscript.

Data availability

Data will be made available on request.

References

Bradley, D., Lau, A., Lawes, M., 1992. Flame stretch rate as a determinant of turbulent burning velocity. Philos. Trans. R. Soc. Lond. Ser. A: Phys. Eng. Sci. 338 (1650), 359–387.

Breitung, W., Dorofeev, S., Kotchourko, A., Redlinger, R., Scholtyssek, W., Bentaib, A., L'Heriteau, J.-P., Pailhories, P., Eyink, J., Movahed, M., Petzold, K.-G., Heitsch, M., Alekseev, V., Denkevits, A., Kuznetsov, M., Efimenko, A., Okun, M., Huld, T., Baraldi, D., 2005. Integral large scale experiments on hydrogen combustion for severe accident code validation-HYCOM. Nucl. Eng. Des. 235 (2), 253–270.

Chan, C., 1995. Collision of a shock wave with obstacles in a combustible mixture. Combust. Flame 100 (1), 341–348.

Dinkelacker, F., Manickam, B., Muppala, S., 2011. Modelling and simulation of lean premixed turbulent methane/hydrogen/air flames with an effective lewis number approach. Combust. Flame 158 (9), 1742–1749.

Dorofeev, S., Kuznetsov, M., Alekseev, V., Efimenko, A., Breitung, W., 2001. Evaluation of limits for effective flame acceleration in hydrogen mixtures. J. Loss Prev. Process. Ind. 14 (6), 583–589.

Dorofeev, S., Sidorov, V., Dvoinishnikov, A., Breitung, W., 1996a. Deflagration to detonation transition in large confined volume of lean hydrogen-air mixtures. Combust. Flame 104 (1), 95–110.

Dorofeev, S., Sidorov, V., Dvoinishnikov, A., Denkevits, A., Efimenko, A., Lelyakin, A., 1996b. Large Scale Hydrogen-Air-Steam DDT Experiments in the RUT Facility. Test Series 1995. Technical Report Report RRC KI 80-05/60, RRC "Kurchatov Institute", Moscow.

Dorofeev, S., Sidorov, V., Dvoinishnikov, A., Denkevits, A., Efimenko, A., Lelyakin, A., 1997. Large Scale Hydrogen-Air-Steam DDT Experiments in the RUT Facility. Test Series 1996. Technical ReportReport RRC KI 80-05/16, RRC "Kurchatov Institute", Moscow.

Dorofeev, S., Sidorov, V., Kuznetsov, M., Matsukov, I., Alekseev, V., 2000. Effect of scale on the onset of detonations. Shock Waves 10, 137–149.

Gaathaug, A.V., Vaagsaether, K., Bjerketvedt, D., 2012. Experimental and numerical investigation of DDT in hydrogen–air behind a single obstacle. Int. J. Hydrog. Energy 37 (22), 17606–17615, HySafe 1.

Gamezo, V.N., Bachman, C.L., Oran, E.S., 2021. Flame acceleration and DDT in large-scale obstructed channels filled with methane-air mixtures. Proc. Combust. Inst. 38 (3), 3521–3528.

Gavrikov, A., Efimenko, A., Dorofeev, S., 2000. A model for detonation cell size prediction from chemical kinetics. Combust. Flame 120 (1), 19–33.

Goodwin, D., 2009. Cantera: an Object-Oriented Software Toolkit for Chemical Kinetics, Thermodynamics, and Transport Processes. Technical Report, Caltech, Pasadena, CA.

Hasslberger, J., Boeck, L.R., Sattelmayer, T., 2015. Numerical simulation of deflagration-to-detonation transition in large confined volumes. J. Loss Prev. Process. Ind. 36, 371–379.

Heidari, A., Ferraris, S., Wen, J., Tam, V., 2011. Numerical simulation of large scale hydrogen detonation. Int. J. Hydrog. Energy 36 (3), 2538–2544.

Kessler, D., Gamezo, V., Oran, E., 2010. Simulations of flame acceleration and deflagration-to-detonation transitions in methane-air systems. Combust. Flame 157 (11), 2063–2077.

Kim, D., Kim, J., 2019. Numerical method to simulate detonative combustion of hydrogen-air mixture in a containment. Eng. Appl. Comput. Fluid Mech. 13 (1), 938–953.

Koike, H., Matsubara, K., 2019. FOCUS-I, Pipeline Fluid Analysis. Technical Report, AdvanceSoft Corporation, URL http://https://www.advancesoft.jp/?s=FOCUS-i.

Kotchourko, A., Lelyakin, A., Yanez, J., Halmer, G., Svishchev, A., Xu, Z., Ren, K., 2015. COM3D: Turbulent Combustion Code. In: Tutorial Guide, Version 4.10. p. 89.

Kuznetsov, M., Alekseev, V., Matsukov, I., Dorofeev, S., 2005. DDT in a smooth tube filled with a hydrogen-oxygen mixture. Shock Waves 14, 205–215.

Kuznetsov, M., Denkevits, A., Veser, A., Friedrich, A., 2022. Flame propagation regimes and critical conditions for flame acceleration and detonation transition for hydrogen-air mixtures at cryogenic temperatures. Int. J. Hydrog. Energy 47 (71), 30743–30756.

Kuznetsov, M., Lelyakin, A., Alekseev, V., Matsukov, I., 2017. Detonation transition in relatively short tubes. In: Ben-Dor, G., Sadot, O., Igra, O. (Eds.), 30th International Symposium on Shock Waves 1. Springer International Publishing, Cham, pp. 481–485.

Kuznetsov, M., Matsukov, I., Alekseev, V., Dorofeev, S., 1999. Photographic study of unstable turbulent flames in obstructed channels. In: Proc. of the 17th International Colloquium on the Dynamics of Explosions and Reactive Systems. ICDERS17, paper 143, pp. 1–4.

Kuznetsov, M., Yanez, J., Grune, J., Friedrich, A., Jordan, T., 2015. Hydrogen combustion in a flat semi-confined layer with respect to the Fukushima-Daiichi accident. Nucl. Eng. Des. 286, 36–48.

Lipatnikov, A., Chomiak, J., 2002. Turbulent flame speed and thickness: phenomenology, evaluation, and application in multi-dimensional simulations. Prog. Energy Combust. Sci. 28 (1), 1–74.

Matsukov, I., Kuznetsov, M., Alekseev, V., Dorofeev, S., 1999. Photographic study of transition from fast deflagrations to detonations. In: Ball, G.J., Roberts, G.T., Hillier, R. (Eds.), Proceedings of the 22nd ISSW. Springer International Publishing, pp. 270–275.

Moen, I., Donato, M., Knystautas, R., Lee, J., 1980. Flame acceleration due to turbulence produced by obstacles. Combust. Flame 39 (1), 21–32.

Nakamori, I., Tomizuka, T., Takahashi, A., Onishi, F., Kuznetsov, M., Kodama, T., Tamauchi, Y., Sato, N., Hayashi, A.K., Tsuboi, N., 2023. Numerical simulation on DDT in real and large scale combustion chamber using a combustion velocity model and ignition model with a detailed chemical reaction system. In: Proc. of the 29th International Colloquium on the Dynamics of Explosions and Reactive Systems. ICDERS29, paper 127, pp. 1–6.

NASA, 1997. Safety Standard for Hydrogen and Hydrogen Systems: Guidelines for Hydrogen System Design, Materials Selection, Operations, Storage and Transportation. Technical Report NASA-TM-112540, Associate for Safety and Mission Assurance, Washington, DC 20546, URL https://ntrs.nasa.gov/citations/19970033338.

Peraldi, O., Knystautas, R., Lee, J., 1988. Criteria for transition to detonation in tubes. Symp. (International) Combust. 21 (1), 1629–1637.

Reynolds, W., 1980. The Element Potential Method for Chemical Equilibrium Analysis: Implementation in the Interactive Program STANJAN. Technical Report, Stanford University, Stanford, CA.

Velikorodny, A., Studer, E., Kudriakov, S., Beccantini, A., 2013. Combustion modeling in large scale volumes. In: Proc. of the International Conference on Hydrogen Safety. ICHS 2013, paper-133, pp. 1–15.

Velikorodny, A., Studer, E., Kudriakov, S., Beccantini, A., 2015. Combustion modeling in large scale volumes using EUROPLEXUS code. J. Loss Prev. Process. Ind. 35, 104–116.

Xiao, J., Breitung, W., Kuznetsov, M., Zhang, H., Travis, J.R., Redlinger, R., Jordan, T., 2017. GASFLOW-MPI: A new 3D parallel all-speed CFD code for turbulent dispersion and combustion simulations Part II: First analysis of the hydrogen explosion in Fukushima-Daiichi Unit 1. Int. J. Hydrog. Energy 42 (12), 8369–8381.

Yáñez, J., Kotchourko, A., Lelyakin, A., Gavrikov, A., Efimenko, A., Zbikowski, M., Makarov, D., Molkov, V., 2011. A comparison exercise on the CFD detonation simulation in large-scale confined volumes. Int. J. Hydrog. Energy 36 (3), 2613–2619.

Yanez, J., Kuznetsov, M., Souto-Iglesias, A., 2015. An analysis of the hydrogen explosion in the Fukushima-Daiichi accident. Int. J. Hydrog. Energy 40 (25), 8261–8280.

Zhang, H., Li, Y., Kuznetsov, M., Jordan, T., Xiao, J., 2019. Numerical study of the detonation benchmark using GASFLOW-MPI. In: Proc. of the 8th International Conference on Hydrogen Safety. ICHS 2019, paper-149, pp. 1–12.